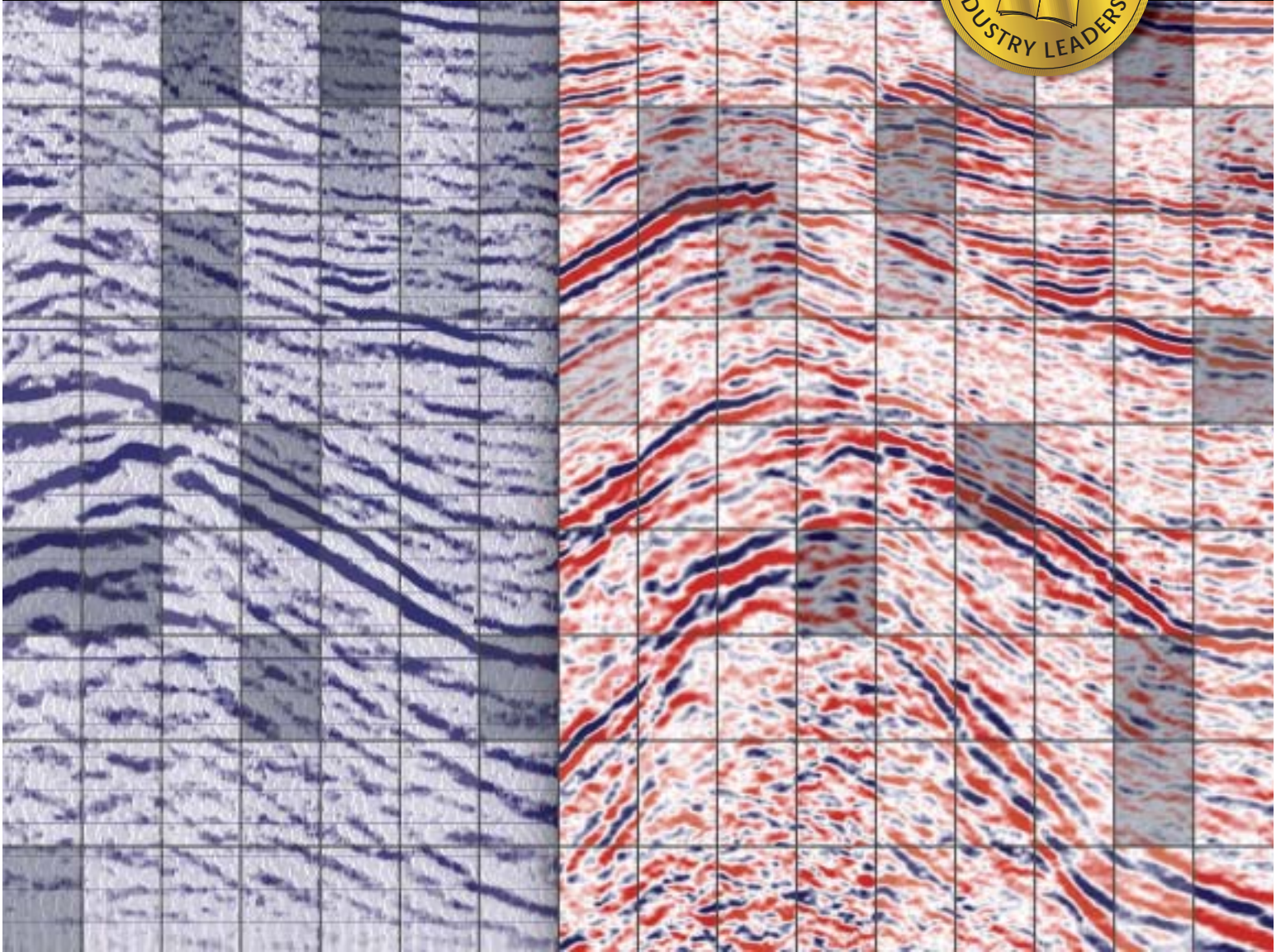


Week of Oct 7, 2002/US\$5.00

PennWell®

OIL & GAS JOURNAL

International Petroleum News and Technology / www.ogjonline.com



COVER

Advances in seismic processing technology can improve imaging of even recently processed seismic surveys. In the side-by-side comparison, the color section displays new seismic imaging that includes the flanks of a salt diapir. The salt flank images were poorly defined in the previous processing, shown on the left in blue and white. An article starting on p. 34 describes curved-ray prestack time migration, the imaging advance responsible for this improvement. Seismic data courtesy of Mayne & Mertz Inc. and Duncan Oil Inc.

Applied Geophysics

Turkmenistan's oil and gas future, Part 1
Design for operational events during well life maintains zonal isolation
NGL fractionation use in W. Canada will increase through 2010
Analysis points to electric-motor drivers for Angola LNG

Curved-ray prestack Kirchhoff time migration is rapidly replacing other seismic time migration methods for focusing seismic images of subsurface structures.

For most geologic environments, curved-ray migration offers tangible imaging improvements over prior time imaging technologies for little additional cost or effort. This trend has a broad significance for members of the seismic industry and their customers because time migration technology is applied to nearly all industry seismic reflection data.

Curved-ray time migration can improve seismic imaging

Walter Kessinger
Geotrace Technologies Inc.
Houston

Seismic time migration

Seismic migration is the culmination of image processing for nearly all exploration seismic surveys. In addition to providing more accurate pictures of subsurface geologic structures, seismic migration products are necessary for reservoir characterization activities such

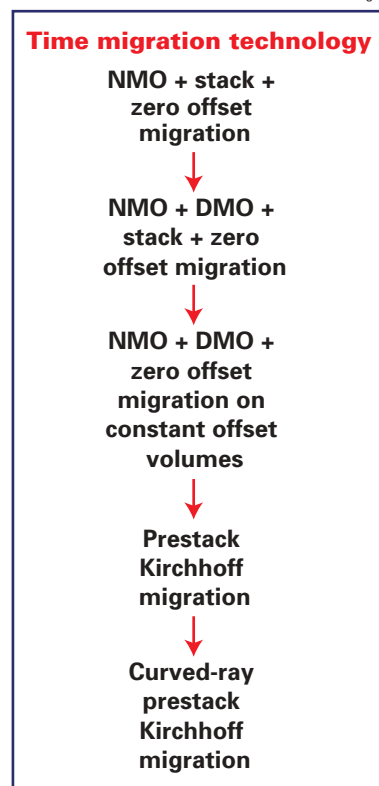


as lithology and fluid prediction, pore pressure prediction, and reservoir volume estimation.

Seismic migration is the term for inverse wave scattering calculations that are used to move seismic reflection images to their position of origin, thereby producing a subsurface image volume. During acquisition of a reflection seismic survey, diffractions and spherical spreading distort the seismic wavefield as it propagates through the subsurface. To produce seismic images that may be interpreted as geologic sections, the seismic data must be transformed by seismic migration.

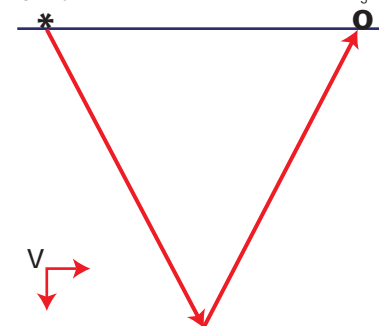
30-YEAR HISTORY

Fig. 1



SEISMIC TRAVEL TIME PATH*

Fig. 2a



*Path for a reflection from a horizontal interface in a constant velocity medium. See equation 2.

Migration methods are classified as either depth migrations or time migrations. This terminology refers to whether the vertical scale of the migrated seismic image is in depth or vertical seismic reflection time. However, the difference between depth migration and time migration is not simply a rescaling of the vertical output axis; depth and time migration algorithms utilize different assumptions about the physics of seismic wave propagation.

Unlike depth migration methods, time migration solutions ignore wavefield distortions created by lateral varia-

GEOMETRIC RELATIONSHIPS*

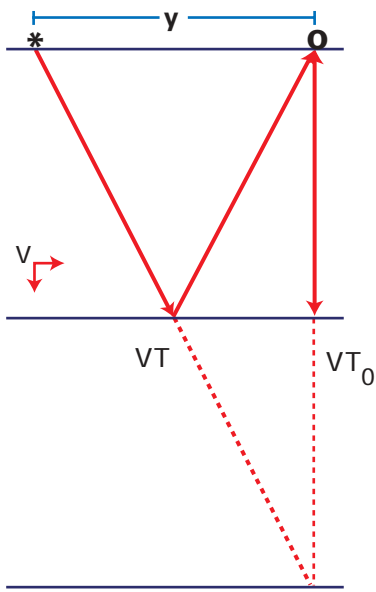


Fig. 2b

*Of variables in equation 2.

tions in seismic velocity. Also, time migration methods usually— but not always—ignore refractions that occur when seismic wavefields cross horizontal velocity boundaries.

Despite these approximations, time migration methods are the dominant imaging tools used in the seismic industry today. The practical advantages of time migration over depth migration are numerous.

For example, depth migration is much more computationally expensive than time migration. Also, the quality of depth migration imaging is more sensitive to the accuracy of the velocity model; depth imaging therefore requires more analysis effort than time migration. Finally, time migration methods are more widely used because time migration technology adequately addresses the seismic imaging needs of many exploration objectives.

Depth migration is traditionally used to address only a specific subset of imaging challenges involving complex geologic structures and complicated seismic velocity fields. And even when these depth imaging objectives are in play, time migration is normally applied before depth migration to develop an initial geologic interpretation and velocity model.

Despite the dominance of time migration over depth migration in current seismic processing practice, technical advances in prestack depth migration have dominated press coverage of seismic processing issues in recent years, both in technical and general interest publications.

This is no doubt because of depth migration's role as the penultimate seismic imaging technology. However, significant improvements have also

EQUATIONS

1. Double square root travel time equation:

$$T = \sqrt{\frac{T_0^2}{4} + \frac{(x + y/2)^2}{v^2}} + \sqrt{\frac{T_0^2}{4} + \frac{(x - y/2)^2}{v^2}}$$

2. Constant velocity moveout equation:

$$T = \sqrt{T_0^2 + \frac{y^2}{v^2}}$$

3. Exact moveout equation for layered media:

$$T = \sqrt{C_0 + C_1 y^2 + C_2 y^4 + \dots}$$

4. Second-order moveout equation:

$$T = \sqrt{T_0^2 + \frac{y^2}{V_{rms}^2}}$$

5. Fourth-order moveout equation:

$$T = \sqrt{T_0^2 + \frac{y^2}{V_{rms}^2} + C_2 y^4}$$

6. RMS velocity equation:

$$V_{rms} = \sqrt{\frac{\sum V_i^2 \Delta t_i}{T_0}}$$

been made in time imaging technology during this same period (Fig. 1). Curved-ray prestack Kirchhoff time migration is the most recent advance in this history.

REFLECTION RAY PATH IN LAYERED MEDIUM*

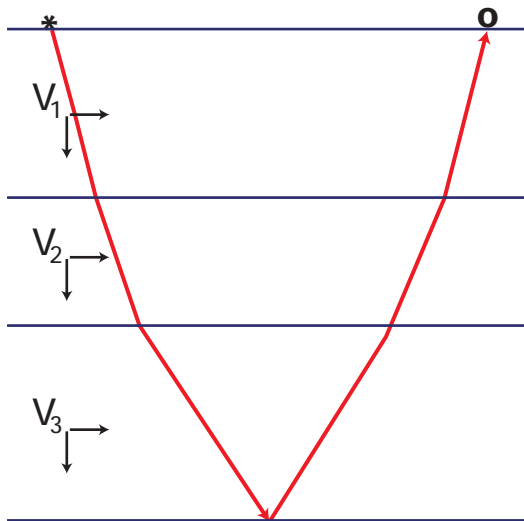


Fig. 3

*P-wave velocities V1, V2, V3 for isotropic constant velocity layers. See equation 3.

SECOND-ORDER STRAIGHT-RAY APPROXIMATION*

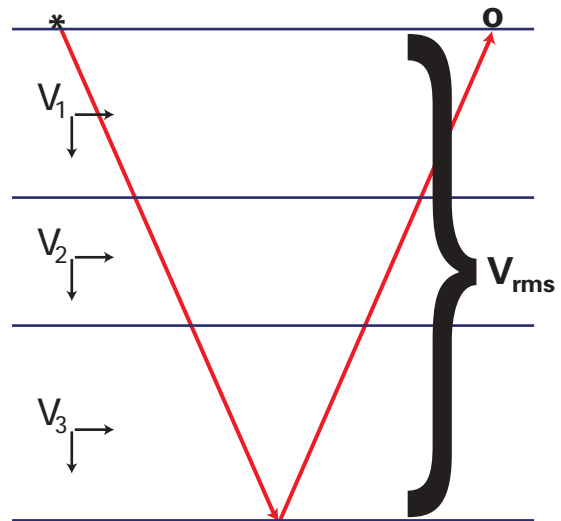


Fig. 4

*For a layered medium. P-wave velocities V1, V2, V3 for isotropic constant velocity layers. See equation 4.

INPUT ZERO-OFFSET SECTION*

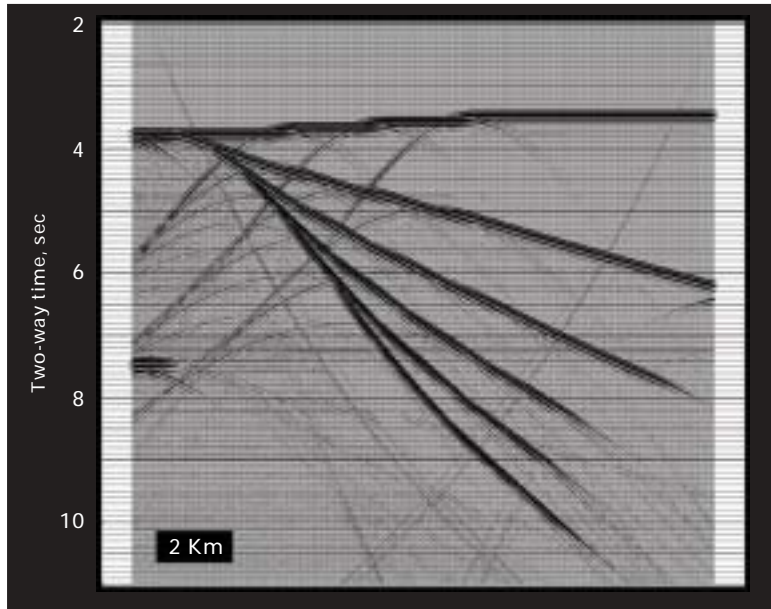


Fig. 5

*From prestack dipping reflector benchmark data.

CURVED-RAY PRESTACK VELOCITY FIELD*

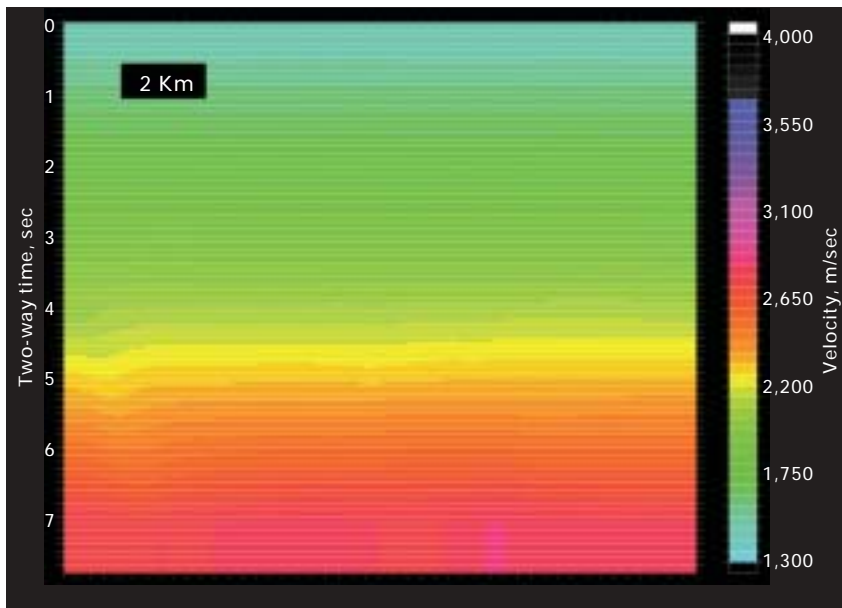


Fig. 6

*Derived using curved-ray prestack time migration and residual moveout analysis.

A significant long-term trend in time migration technology has been the elimination of the zero-offset approximation (Fig. 1). Zero-offset migration is based on the assumption that the seismic source and receiver occupy the same physical location during acquisition of seismic data.

The symmetries introduced into the migration operation by this assumption

reduce its computational requirements by orders of magnitude. However, because each trace of a seismic record actually has a nonzero source-receiver offset, this approximation requires preprocessing steps such as normal moveout, dip move-out, and stack.

The intent of these operations is to replace the acquired seismic data with data that approximate seismic experi-

ments that were never actually conducted. Because each of these operations requires its own simplifying assumptions, additional errors are introduced into the imaging process with each additional procedure.

Today, the zero-offset migration approximation plays a minor role in seismic processing practice due to the routine application of prestack Kirchhoff time migration. The production use of Kirchhoff time migration has been made possible by continuous improvements by the computer industry in computer performance and speed. However, standard Kirchhoff time migration still retains another limiting approximation: the assumption that seismic energy traveled through the subsurface at a constant velocity.

This constant velocity assumption is known as the straight-ray approximation. Curved-ray prestack time migration extends the accuracy of Kirchhoff time migration by explicitly accounting for ray path bending due to variation in seismic velocity with depth.

Ray paths

To appreciate the advance represented by curved-ray prestack time migration, it is first necessary to examine the mechanisms and approximations of standard prestack Kirchhoff time migration.

Equation 1 is known in exploration seismology as the double-square root equation.¹ The 2D version of this equation is presented for simplicity.

This equation describes Cheop's pyramid, the travel-time surface of reflections in prestack seismic data from a single point diffractor. Given a point diffractor at depth z , if the seismic velocity V is assumed constant in the subsurface, then the two-way vertical seismic travel-time between the point diffractor and the surface location immediately above it is given by T_0 , where $T_0 = 2z/V$.

If y is the source-receiver offset, and x is the horizontal distance from the diffracting point to the source-receiver midpoint, then equation 1 describes the travel time from any source location on the surface to the point diffractor to a surface receiver position—for a constant velocity earth.

Fig. 2a shows a seismic ray path in a



constant velocity medium where the reflection point lies directly underneath the source-receiver midpoint. The travel-time in this special situation is given by equation 2, the normal move-out equation for a constant-velocity medium. Equation 2 is actually a special case of the travel-time equation given in equation 1 with $x=0$. Fig. 2b is a graphic representation of the geometrical relationships for this case.

Of course, the constant velocity medium shown in Fig. 2 is an unacceptably oversimplified earth model for seismic processing purposes. A better approximation of the earth's near subsurface (Fig. 3) is composed of homogeneous horizontal layers with interval velocities V_1, V_2, V_3 , and so on. This is the most ambitious model type that time migration aspires to correctly image; by definition, solving for distortions caused by lateral velocity variations would be depth migration.

The complete analytical normal move-out equation for travel-times in a layered earth has been derived by Taner and Koehler² and is presented in equation 3. The form of this equation is an infinite Taylor series expansion in even powers of y .

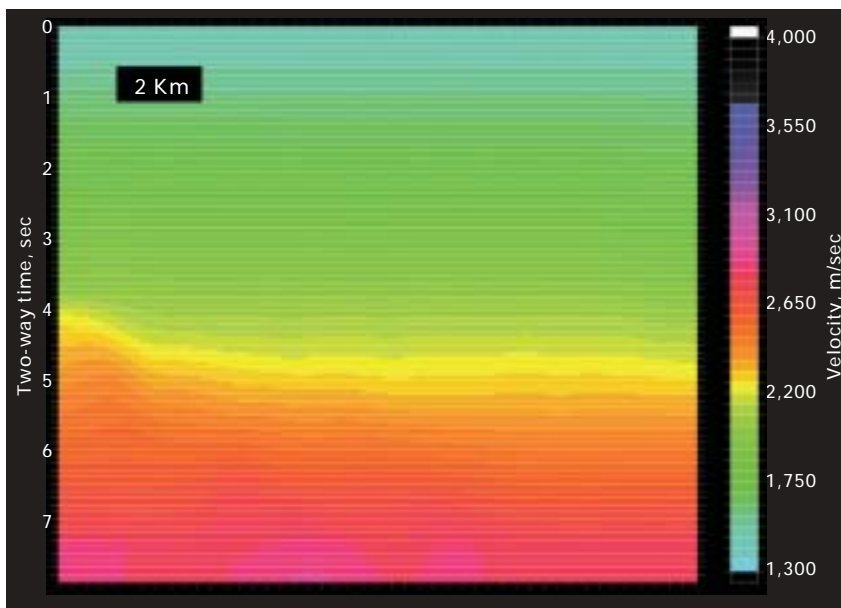
The coefficients C_0, C_1, C_2 , and so on, are functions of the layer thicknesses and interval velocities. In fact, the first two terms, C_0 and C_1 , are T_0^2 and $1/V_{rms}^2$, respectively, where V_{rms} is the root-mean-square velocity between the surface and the reflector. By truncating equation 3 after the second term, therefore, the second-order hyperbolic move-out equation is obtained (equation 4).

In addition to being the basis of normal move-out and stacking velocity analysis, the second-order move-out equation is also intimately related to prestack time migration. Comparison of equations 2 and 4 show that they have identical form. By substituting V_{rms} into equation 1, we obtain the double-square-root equation that is the basis of standard Kirchhoff time migration.

Prestack Kirchhoff time migration produces the migrated image at a single subsurface point by summing together all the seismic reflection samples in a survey that are described by this surface. A migrated image volume is constructed by recalculating Cheops pyra-

STRAIGHT-RAY PRESTACK VELOCITY FIELD*

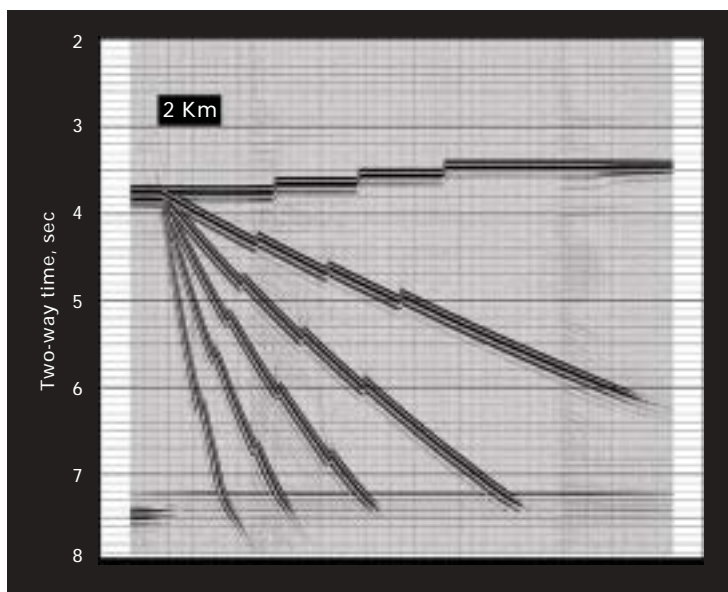
Fig. 7



*Derived using straight-ray prestack time migration and residual moveout analysis.

CURVED-RAY PRESTACK MIGRATION IMAGE*

Fig. 8



*Using optimum curved-ray imaging velocities. Velocity field derived using curved-ray prestack time migration and residual moveout analysis.

mid and repeating this operation for every subsurface location in the volume of interest.

It is of special interest that although the RMS velocity field varies spatially, we are applying a constant-velocity approximation at every point when we use a second-order equation as the basis of our prestack time migration (Fig. 4). This is why standard prestack Kirch-

hoff time migration is also referred to as straight-ray time migration.

There are several ways in which prestack Kirchhoff time migration can be extended to accommodate ray curvature. The most straightforward method is to preserve higher-order terms from equation 3 in the migration operator (equation 5¹). Another approach is to ray trace the one-dimen-

STRAIGHT-RAY PRESTACK MIGRATION IMAGE*

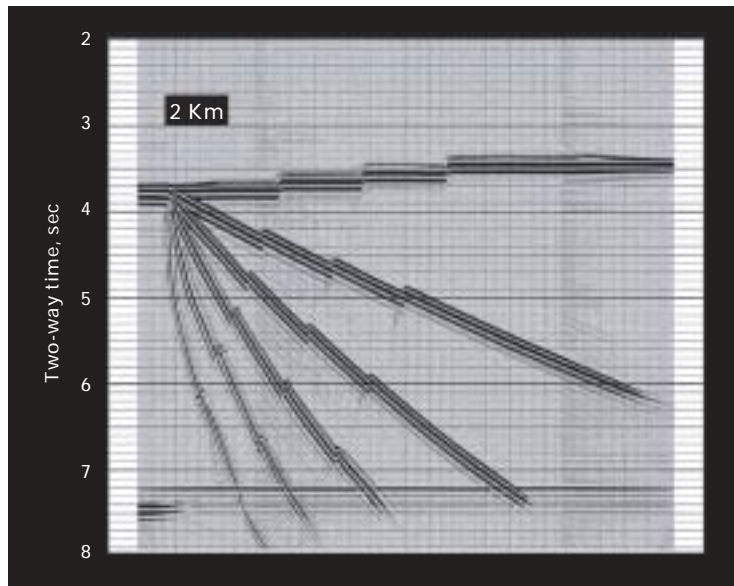


Fig. 9

that the accuracy of the method will still be limited by the time migration methodology.

At some point, errors inherent in ignoring lateral velocity variations in the subsurface will be greater than the incremental gains in accuracy achieved by adding additional high-order terms to the time migration operator.

Steep dip imaging

Straight-ray migration introduces two distinct errors into the imaging process by ignoring ray path curvature.

The first error is the error in vertical move-out for long offset data, described in the previous section. For reflectors with negligible dip, this move-out error can be partially corrected either by application of an optimized imaging velocity or by applying a residual high-order move-out correction after migration. For reflectors without dip in media with no lateral velocity variation, the lateral positioning of the reflectors is correct after migration, so residual move-out is an acceptable and accurate correction.

For dipping events, however, straight-ray migration introduces an additional error in positioning—a lateral positioning error. Furthermore, this lateral positioning error varies with both dip and offset, making it more difficult to correct for the shortcomings of the straight-ray method with either “optimized” migration velocities or post-migration compensations.

The problem of imaging dipping reflectors with straight-ray methods is illustrated here with synthetic 2D prestack seismic data that were created using wave equation modeling. Fig 5 shows the unmigrated zero-offset section from the full prestack data set. The model includes reflectors with dips of 0° (with vertical faults), 15°, 30°, 45°, 60°, and 75°, as well as a weak horizontal reflector at 5.2 sec. The velocity model used to generate the data varied with depth only, but it was not provided as part of this curved-ray migration benchmark.

Migration velocities were derived using iterative time migration and residual velocity analysis on the dipping reflector synthetic. The velocity field shown in Fig 6 was derived using a fourth-order curved-ray time migra-

*Using optimum straight-ray imaging velocities. Velocity field derived using straight-ray prestack time migration and residual moveout analysis.

CURVED-RAY PRESTACK MIGRATION IMAGE*

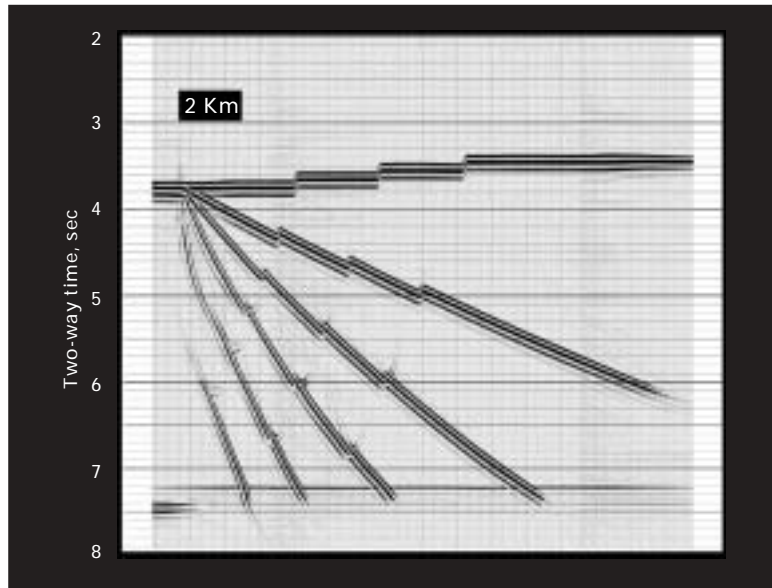


Fig. 10

*Using straight-ray derived velocities (Fig. 7). Velocity field derived using straight-ray prestack time migration and residual moveout analysis.

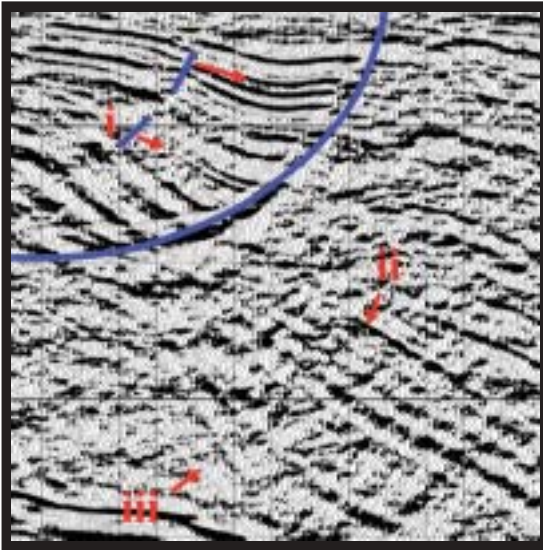
sional layered earth model that is the basis of imaging at every CMP location (but is free to vary from one CMP location to the next).

Because the time migration velocity field is normally composed of RMS velocities derived by some form of move-out analysis, either of these approaches requires that interval velocities be inverted from the interpreted RMS veloci-

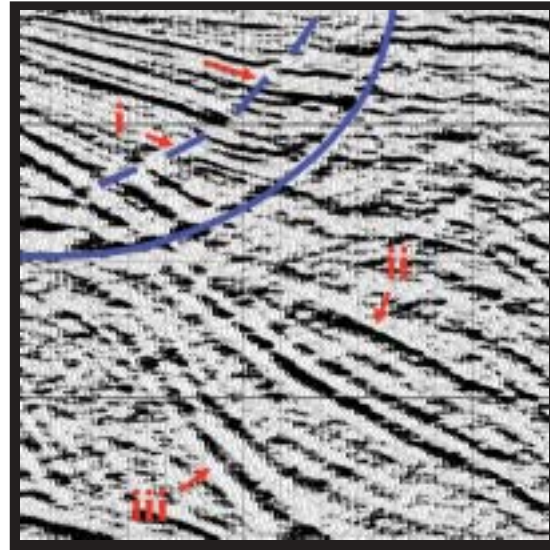
ties. This operation is usually accomplished on the fly during the time migration.

The ray tracing solution described above is equivalent to preserving all terms of the infinite Taylor series in equation 3. Although it is possible and economically feasible to construct an arbitrarily high-order curved-ray migration, it is advisable to keep in mind

A Straight-ray prestack Kirchhoff time migration.



B Curved-ray prestack Kirchhoff time migration.



Source: Data provided courtesy of Duncan Oil Inc., Houston and Denver.

tion, and the velocity field shown in Fig. 7 was derived using straight-ray time migration.

At 5 sec on the vertical axis, the velocity values from the two methods differ by 2% on the right side of the section and by more than 8% on the left side of the section. The lateral variation in the derived migration velocities is much more pronounced in the straight-ray results than in the curved-ray results.

This velocity variation is a consequence of the straight-ray “best compensation velocity” being a function of dip and is an expression of the increasing reflector dip in the section from right to left.

The reflector images obtained by the two migrations are shown in Figs. 8 and 9. Both migrations produce crisply imaged reflectors, even for the steepest events. However, positioning differences between the two methods increase with increasing dip; the 75° dipping reflector actually appears slightly overturned in the straight-ray migration image.

The significance of these imaging errors should be self-evident to any explorationist who has ever been concerned with positioning a well near the flank of a salt diapir.

A final test was conducted using the curved-ray migration with the velocity

model derived from the straight-ray processing sequence. The results (Fig. 10) demonstrate the problems in imaging using an inappropriate migration velocity field.

As with the straight-ray migration, the migrated reflectors are mispositioned and distorted. Moreover, because the migration velocities are not optimum for the curved-ray migration algorithm, the steepest reflector in the section is no longer coherently imaged.

Field data examples

As with the synthetic benchmark in the last section, comparisons of straight-ray migration and curved-ray migration on field data require that the appropriate migration velocities be derived independently for each method.

Unlike the synthetic benchmark, the true answer for field data is unknown for either the velocities or the migrated image. However, because of the theoretical improvements in curved-ray prestack time migration, it is reasonable to expect that the velocities derived by this method are a better approximation of the true earth velocities, and that the curved-ray migration should produce superior positioning of dipping reflectors.

Fig. 11 shows a field data comparison of straight-ray (11a) and curved-ray (11b) migrations imaging a growth

fault structure in Southeast Texas. In this comparison, the apparent location of a minor fault that runs parallel to the interpreted major fault changes dramatically in the two images (i), and the dips and continuity of reflectors beneath the fault are substantially altered (ii and iii).

The final example makes the point that seismic processing practices have improved in areas other than just migration imaging. When a field survey is reprocessed to update straight-ray migrated results with curved-ray migration, it is frequently the case that the imaging also benefits from improvements in the pre-migration processing.

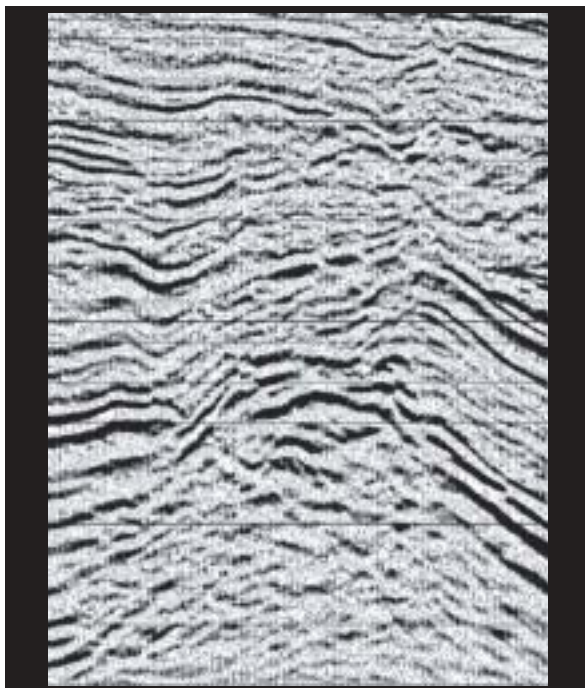
This would certainly seem to be the case in the Southwest Louisiana example shown in Fig. 12. The curved-ray migration results (Fig. 12b) exhibit obvious improvements over the previous straight-ray migration imaging (Fig. 12a) in the definition of faults in the upper portion of the section and in the steep-dip imaging associated with the diapir structure at the bottom of the section.

Although some of this improvement is undoubtedly due to inherently better imaging by curved-ray prestack time migration, much of the improvement is likely the result of advances in automatic first-break picking, which led to better geometry and statics processing,

COMPARISON OF FLANKS OF SW LOUISIANA SALT DIAPIR

Fig. 12

A Previous processing, including straight-ray prestack Kirchhoff time migration.



B Updated processing, including curved-ray prestack Kirchhoff time migration.



Source: Data provided courtesy of Mayne & Mertz Inc., Houston and Midland.

and improved amplitude preservation throughout the processing sequence.

The outcome

In conclusion, imaging results with curved-ray prestack Kirchhoff time migration have confirmed expectations of better steep dip and fault plane imaging than standard prestack Kirchhoff time migration.

In addition, tests with computational data indicate that migration velocities derived using curved-ray migration should be better estimates of subsurface seismic properties than velocities from other time migration methods.

Because curved-ray Kirchhoff time migration involves as little as 20% additional computational effort than straight-ray Kirchhoff time migration, it is likely that curved-ray migration technology will completely replace straight-ray methods in the immediate future.

Acknowledgments

Thanks to Duncan Oil Inc., Denver and Houston, for permission to present the Southeast Texas field data example and Mayne & Mertz Inc., Midland and Houston, for permission to show the growth fault field data in Fig. 12. Mark Chang of BP America Inc. provided the dipping reflector synthetic used for curved-ray migration testing. Thanks to co-workers at Geotrace Technologies Inc. whose work contributed to this article: Bob Wojslaw, who authored the Kirchhoff time migration software used in the examples in this paper and who produced the study of the dipping reflector synthetic; John Makin, who provided the notes and illustrations used to construct the discussion on move-out and travel time operators; and Karen Chevis and Bert Macy, the geophysicists who produced the field examples used here.

References

1. Yilmaz, Ozdogan, "Seismic Data Analysis," Vols. 1 and 2, Society of Exploration Geophysicists, Tulsa, Okla., 2001.
2. Taner and Koehler, "Velocity spectra—Digital computer derivation and applications of velocity functions," *Geophysics*, 1969, pp. 859-881. ♦

The author

Walter Kessinger (wkessinger@geotrace.com) is a senior research geophysicist with Geotrace Technologies Inc. With 15 years of experience in seismic imaging, he spent 9 years at the Houston Advanced Research Center, where he was the coordinator of an industry-sponsored seismic imaging research consortium. He holds an MA in geophysics from the University of Texas at Austin and a BS in physics from Louisiana State University.



GEOTRACE

www.geotrace.com

Houston, Texas USA
+1 281-497-8440

Dallas, Texas USA
+1 972-690-1122

Tolworth, Surrey UK
+44 (0) 20-8406-4660

Weybridge, Surrey UK
+44 (0) 1932-857433

Stavanger, Norway
+47 51-87-4520